Published in final edited form as:

Curr Biol. 2023 December 04; 33(23): 5233–5239.e3. doi:10.1016/j.cub.2023.10.027.

A time memory engram embedded in a light-entrainable circadian clock

David E. Ehichioya[1],

S. K. Tahajjul Taufique[1],

Sofia Farah,

Shin Yamazaki[*]

Department of Neuroscience and Peter O'Donnell Jr. Brain Institute, UT Southwestern Medical Center, 5323 Harry Hinds Blvd., Dallas, Texas 75390-911, U.S.A.

SUMMARY

A longstanding mystery in chronobiology is the location and molecular mechanism of the food-entrainable oscillator (FEO)[1–3]. The FEO is an enigmatic circadian pacemaker that controls food anticipatory activity (FAA). The FEO is implicated as a circadian oscillator that entrains to feeding time. However, the rhythmic properties of the FEO remain a mystery in part due to technical limitations in distinguishing FAA from locomotor activity controlled by the primary circadian pacemaker in the suprachiasmatic nucleus (SCN). To overcome this limitation, we used the Feeding Experimentation Device version 3 (FED3) to measure food-seeking nose poking behavior. When food availability was limited to 4h at night, mice exhibited strong anticipatory nose poking behavior prior to mealtime. When food availability was moved to the daytime, mice quickly expressed daytime anticipatory nose pokes without displaying transients. Unexpectedly, the mice also maintained nighttime anticipatory nose pokes, even though food pellets were no longer dispensed at night. We next tested if food anticipation was directly encoded on a light-entrainable oscillator by shifting the light-dark cycle without changing mealtime. Anticipatory behavior shifted in parallel with the light-dark cycle, even though meal timing was unchanged. Next, we tested whether encoding meal timing for anticipatory nose pokes required a functional SCN by studying *Period 1/2/3* triple knockout mice with disabled SCN. Food anticipatory nose poking of *Period* knockout mice shifted in parallel with the light-dark cycle independent of a functional SCN clock. Our data suggest that food anticipation time is embedded in a novel, extra-SCN light-entrainable oscillator.

[*]Corresponding author: shin.yamazaki@utsouthwestern.edu.

[1]Equal contribution

AUTHOR CONTRIBUTIONS

Conceptualization, D.E.E, S.K.T.T., S.F. and S.Y.; Formal Analysis, D.E.E, S.K.T.T., and S.Y.; Investigation, D.E.E, S.K.T.T. and S.F.; Writing – Original Draft, S.Y.; Writing – Review & Editing, S.F. and S.Y.; Supervision, S.Y.; Funding Acquisition, S.Y.

DECLARATION OF INTERESTS

The authors declare no competing interests.

eTOC Blurb

The prevailing view is that the food-entrainable oscillator does not entrain to light. Ehichioya et al. measured food anticipatory nose-poking behavior and found that the time of nose-poking behavior entrained to the environmental light-dark cycle, even in mice lacking functional molecular timekeeping in the suprachiasmatic nucleus.

RESULTS

Time of food anticipation was encoded to a light-entrainable circadian oscillator

Since Richter first reported FAA in rats in 1922[4], many studies have attempted to reveal the fundamental mechanisms of the FEO[3]. Stephan and others showed that FAA is a bona fide circadian rhythm because it persists in constant conditions (e.g., fasting) and is entrainable, as evidenced by transients when re-entraining to shifted feeding schedules[5,6]. Studies also made shocking discoveries that the FAA rhythm persists in SCN-lesioned rodents and the mutant mice lacking functional circadian genes have normal FAA rhythms[3]. Therefore, studying the FEO provides a unique opportunity to discover a novel circadian timekeeping mechanism in a pacemaker outside of the SCN. A challenge in FEO research is that FAA, which is the observable rhythmic locomotor activity output of the FEO, is often indistinguishable from locomotor activity controlled by the SCN. Recently, Mistlberger and colleagues showed that lever pressing and nose poking are outputs of the FEO[7]. This motivated us to use an open-source feeding device, the FED3[8], to measure food-seeking nose poking behavior during temporally restricted feeding.

C57BL/6N male mice were singly housed with a running wheel in a 12h light: 12h dark condition. Food pellets (20mg each) were dispensed from the FED3 when the mice poked their noses into one of two nose holes (no other food was available). We programmed the FED3 to dispense 1 pellet in response to a left nose poke, but not to a right nose poke. We first recorded food-seeking behavior in *ad libitum* feeding conditions where the mice were rewarded with a food pellet after a left poke at any time of day. Within the first 2 days of *ad libitum* food availability, all C57BL/6N mice learned to dispense a pellet by left nose poking. Mice normally took ~200 pellets per day during *ad libitum* feeding (Figure S3). Consistent with prior studies[9,10], the mice ate ~75% of their food during the night. Importantly, there was no consolidated nose poking or pellet intake during *ad libitum* feeding (Figure 1).

Next, we placed mice on a timed food restriction schedule where mice received pellets only for 4h at night. We gradually reduced the food availability window from 8h to 4h. Within a few days of beginning 8h restricted feeding, mice already had frequent intense consolidated nose pokes from ~4h before the onset of the scheduled feeding time until pellets were dispensed (Figure 1, S1). Most mice expressed both left and right anticipatory pokes, but rewarded left anticipatory poking was stronger (Figure 1, S1, S3A–D). Anticipatory wheel running activity was not observable because it was masked by the SCN-controlled nocturnal activity.

To test the food-entrainability of the anticipatory poking rhythm, we shifted the feeding window from the nighttime to the daytime by 12h. Based on a prior study, we expected to observe transients of nose-poking behavior as it gradually shifted to the daytime. Unexpectedly, we observed that mice immediately started expressing anticipatory poking for the daytime meal within 2 days of imposing the new feeding time (Figure 1, S1). Remarkably, in addition to the daytime anticipatory poking that resulted in the food reward, mice also continued to have frequent left nose pokes consolidated at the time of the previous nighttime meal for 2 weeks, even though mice no longer received pellets at night (Figure 1, S1). If the FEO had entrained to the new feeding time, then the nighttime pokes should not have persisted.

Because there were only two 24h environmental signals, light and food, we hypothesized that mice anticipated the new time of food availability by adding a “food timestamp” to a circadian oscillator entrained to light. To test this, we advanced the light-dark cycle by 6h while the feeding schedule was held unchanged. The onset of daytime anticipatory nose pokes gradually advanced, while unrewarded nighttime anticipatory poking gradually disappeared (Figure 2A). When we delayed the light-dark cycle by 9h, we saw a striking effect on anticipatory pokes such that they rapidly delayed ~9h within 2 days of delaying the light-dark cycle (Figure 1, S1). The anticipatory pokes to the scheduled food availability temporarily damped and then reappeared ~3–6 days after the light-dark cycle shift (Figure 1A, 2D, S1). Wheel running activity exhibited both SCN-controlled activity and food anticipatory activity. Food anticipatory wheel running activity mirrored anticipatory left nose poking measured by the FED3. Quantitative analysis revealed the onset of anticipatory nose pokes shifted slightly faster than SCN-controlled onsets of wheel activity to advances and delays of the light-dark cycle (Figure 2 B, C, E, F).

Analysis of daily pellet intake revealed that pellet intake decreased shortly after changes in the timing of feeding and the lighting schedule (Figure S3B). The largest pellet intake reduction was observed shortly after food availability moved from nighttime to daytime by 12h (Figure S3B–II). This drop in pellet intake gradually recovered to the baseline level by ~14 days. Interestingly, this coincides with the approximate day when anticipatory poking for unrewarded previous mealtime disappeared (Figure 1, S1). The second largest pellet intake drop was observed after the light-dark cycle was delayed by 9h (Figure S3B–IV). Interestingly, changes in wheel running activity, and rewarded left and unrewarded right nose pokes were in the opposite direction (Figure S3). Changes in the feeding or light-dark schedules temporarily suppressed pellet intake. In contrast, wheel running activity and nose poking were increased (note, increased wheel running one day before feeding time was likely due to a cage change, see Figure S1 for individual actograms). These data suggest that caloric food restriction may be necessary to continue to express anticipatory nose poking at the previous time of food availability. This is consistent with the well-defined observation that food anticipatory activity continues during food deprivation but immediately disappears during *ad libitum* feeding[3,5,6].

Mice without functional SCN still exhibit light entrainment of food anticipation

We next performed the experiment with mutant mice that have no functional SCN. Because SCN-lesioned rodents are rarely rhythmic under the light-dark cycle, due to disruption of retinal projections to the brain [11–15], studying SCN-lesioned mice was not a feasible approach to test light entrainability. Therefore, we used *Period1/2/3* triple knockout mice (*Per1/2/3* KO), because unlike SCN-lesioned mice, they have robust daily activity rhythms in the light-dark cycle, with activity onset ~2 h before lights off[16]. Some have assumed that this apparent rhythm is due to masking by light or is controlled by a light-driven SCN oscillation. To test whether the SCN is rhythmic, we crossed *Per1/2/3* KO mice with *c-fos*-short half-life variant green florescence protein (shGFP) reporter mice and measured *c-fos*-shGFP expression in the SCN during the day and night. We observed only sparse GFP-expressing SCN neurons in the middle of the day and the middle of the night in *Per1/2/3* KO mice (Figure 3B). This was in striking contrast to GFP expression in wildtype mice, which have robust day-night differences in the number of GFP expressing neurons in the SCN (Figure 3A). These data suggest that the SCN is not rhythmic in *Per1/2/3* KO mice and therefore the SCN cannot be responsible for activity rhythms in these mice under the light-dark cycle. This provided us with the unique opportunity to assess light entrainablity of food anticipation without a functional SCN clock (Figure 4, S2). Similar to wildtype mice, all male *Per1/2/3* triple KO mice learned to dispense pellets within 2 days in *ad libitum* feeding and expressed anticipatory nose pokes to nighttime restricted feeding. After advancing the light-dark cycle by 9h, anticipatory nose poking advanced immediately, while anticipation of the unchanged nighttime mealtime temporarily disappeared and then gradually reappeared again (Figure 4). Phase-advanced anticipatory nose poking of most *Per1/2/3* KO mice was not as stable as in wildtype mice. Unlike wildtype mice, both onsets of wheel running activity and anticipatory nose poking were advanced rapidly in synchrony with the advanced light-dark cycle (Figure 4 C, D). Similar to wildtype mice, both daily rewarded left poking and unrewarded right poking in *Per1/2/3* triple KO mice increased drastically when mice were exposed to nighttime restricted feeding (Figure S3G, H). Although advancing the light-dark cycle immediately suppressed pellet intake, rewarded left nose poking didn't increase until 4 days after changing the light-dark cycle (Figure S3G). The daily total of wheel running activity or unrewarded right nose pokes were minimally affected by the advancing light-dark cycle (Figure S3E, H).

DISCUSSION

The anatomical location and timekeeping mechanism of the FEO is one of the remaining mysteries of circadian biology. Efforts to identify the locus of the FEO using brain microlesions resulted in a long list of brain regions that are not required for FAA[1,2]. This led to a new working model that the FEO is housed in a distributed network throughout the brain and/or body[5]. Another approach is that researchers have tried to map the locus of the FEO by searching for brain areas that exhibit phase-changes during restricted feeding[17]. Both approaches have been unsuccessful in discovering the locus of the FEO for the last 50 years. The results of our current study, suggesting that FAA is marked on a light-entrainable oscillator, could account for the futility of the prior studies searching for the FEO. Prior studies of FAA were limited because activity is an output of both the SCN and the food-

entrainable oscillator(s). Inspired by the pioneering studies of Mistlberger and his colleagues using lever pressing paradigms during temporally restricted feeding, we sought to develop an assay that measured food-seeking behavior that was distinct from outputs of the SCN. We adapted the FED3 system to measure food-rewarded nose poking behavior anticipating mealtime during temporally restricted feeding, similar to FAA. This gave us a new tool to probe the mechanisms of food anticipatory behavior.

Several lines of evidence in the current study suggest that the timing of meals is encoded in a light-entrainable oscillator, which in turn controls food anticipatory behaviors. First, after mealtime was shifted, wildtype mice continued to anticipate their prior mealtime, even though food was not presented at the time of the prior meal. Second, when the light-dark cycle was advanced by 6 hours, the onset of anticipatory nose poking gradually phase advanced in concert with the gradual advance of the SCN-controlled activity. During this experiment, mice had an extended duration of anticipatory nose poking behavior. Since food availability continued at the same time, we hypothesize this long duration anticipatory behavior encompasses anticipation of two mealtimes-the mealtime that was perceived as shifted when the light-dark cycle shifted and the current time of food availability (which was not shifted). Third, there were two distinct anticipatory nose poking bouts after 9h delays of the light-dark cycle. Phase delays of a light-entrainable oscillator are rapid so the mealtime marked on the light-entrainable oscillator rapidly delayed and was distinct from the time of food availability.

Previous studies showed that the light-entrainable SCN was not required but participated in food anticipation[15,18]. To remove influences of the SCN, we used *Per1/2/3* KO mice with disabled SCN rhythmicity. We found that *Per1/2/3* KO mice exhibited anticipatory poking to nighttime meals. This anticipatory poking shifted in concert with the light-dark cycle. While wildtype mice with functional SCN had gradual light entrainment (i.e., transients) of food anticipatory activity (nose poking and wheel running) and SCN-controlled nocturnal activity, *Per1/2/3* KO mice had instant phase advances of their food anticipatory nose poking that paralleled the change in the environmental light-dark cycle. Anticipatory nose poking in *Per1/2/3 KO* mice was not stable as that seen in wildtype mice and there were large cycle-to-cycle deviations in phases of both anticipatory nose poking and wheel activity. This was particularly evident for several days after advancing the light-dark cycle. The period of the FEO in *Per1/2/3* KO mice was previously estimated as ~21h[16]. To entrain this short-period oscillator to the 24h light-dark cycle, the FEO needs to delay ~3h every day. Perhaps this is the reason why advanced anticipatory poking was unstable.

Our current study is consistent with a firmly established consensus that the SCN is not required for food anticipatory behavior and further suggests that mice use an extra-SCN light-entrainable oscillator to anticipate the time of food availability. However, our study does not exclude the possibility that this oscillator can entrain to feeding time in the absence of a light cue. Stephan showed that food anticipatory activity in SCN-lesioned rats gradually re-entrained to a shifted feeding schedule with a few days of transient cycles[19]. Our current study shows that if both light and food cues are present, light is the dominant environmental cue that entrains this oscillator. When mealtime was changed, mice immediately anticipated the new feeding schedule by adding a new food timestamp to the light-entrainable oscillator

rather than entraining to the new feeding time. As a result, mice temporarily exhibited two anticipatory events which reflect both current and previous feeding times without showing transients (Figure S4). We previously showed that *Per1/2/3* KO mice exhibited robust FAA when mice were fed on a 21h, but not 24h, feeding cycle under constant darkness[16]. Therefore, it is likely that the FEO can entrain to feeding cycles with periods closer to its autonomous period in the absence of a functional SCN or without environmental light-dark cycles. In contrast, in the presence of the 24h light-dark cycle, *Per1/2/3* KO mice can anticipate a 24h feeding cycle. This suggests that light is a primary environmental cue that entrains the extra-SCN circadian oscillator in *Per1/2/3* KO and that it can entrain to a 24h light-dark cycle, but not to a 24h feeding cycle.

Previous studies showed that rodents can anticipate multiple mealtimes, which serves as evidence for the existence of multiple FEOs in rodents[7,20–22]. If each FEO couples to the light-entrainable oscillator with a different strength, most of the results of our current study can be explained by this multi-FEO model[7]. A recent study showed that SCN-lesioned rats exhibited two different periods of food anticipation when rats were given two different periods of feeding schedule. Those two different periods of food anticipation persisted under food deprivation[7]. Although our model (Figure S4C) is the simplest way to explain our results as well as previous studies of multiple mealtime anticipation, our model cannot explain this multi-period food entrainment. Therefore, the chronoarchitecture of food anticipation is likely more complex and should be further investigated. Nevertheless, our study provides a novel technological approach and conceptual framework for future studies searching for the elusive FEO.

STAR*METHODS

RESOURCE AVAILABILITY

Lead contact—Further information and requests for resources and reagents should be directed to and will be fulfilled by the lead contact, Shin Yamazaki (shin.yamazaki@utsouthwestern.edu).

Materials availability—This study did not generate new unique reagents.

Data and code availability—All raw ClockLab and FED3 data and original codes have been deposited to Mendeley Data, V1, doi: 10.17632/cr5hkkdtx2.1

Analyzed data and confocal images reported in this paper will be shared by the lead contact upon request.

Any additional information required to reanalyze the data reported in this paper is available from the lead contact upon request.

EXPERIMENTAL MODEL AND STUDY PARTICIPANT DETAILS

Mice—Adult mice from the breeding colony at UT Southwestern Medical Center were used in this study. All experiments were carried out in accordance with the National Institutes of Health Guidelines regarding the care and use of animals for experimental procedures and

were approved by the Institutional Animal Care and Use Committee at UT Southwestern Medical Center (Protocol #: 2016–10376-G).

METHOD DETAILS

Eight adult male C57BL/6N mice (165-day-old) and 6 *Per1/2/3* KO male mice (C57BL/6J background, 67 to 180-day-old)[16,23–25] were individually housed in a large cage (16.0 cm W, 32.0 cm L, 12.5 cm H) with woodchip bedding (Sani-Chips, PJ Murphy Forest Products). A running wheel (11.0 cm diameter) attached to the cage lid was used to monitor wheel-running activity. Magnetic switch-activated wheel running revolutions were recorded every 1 min by ClockLab (ver. 3.604, Actimetrics). All cages were placed inside light-tight cabinets and temperature, humidity, and light intensity inside of the cabinet were recorded every 5 min by Chamber Controller software (ver. 4.104, Actimetrics). The white LEDs inside the cabinet were controlled by the Chamber Controller software and light intensity inside the cage was ~100 lux during the light phase. Actual lights-on and lights-off times inside the cabinets were detected by cds cells and recorded by ClockLab. The FED3 was placed inside the cage and the time of pellet intake, right nose poke, and left nose poke were recorded on the SD card inside the FED3. A 20 mg food pellet (Rodent Grain-Based Diet # F0163, Bio-Serv) was dispensed in response to a left nose poke and was the only source of food for the mice during the experiment. We disabled the LED lights and buzzer of the FED3 so there was no cue associated with food availability. We also programmed the FED3 such that the right nose poke did not dispense a food pellet. Therefore, the only way for mice to know the food was available was by poking in the left nose poking hole and/or time memory for the time window when food was available. Water was always available during the experiment. We visually inspected the FED3 and pellet intakes daily. Food pellets were refilled in the FED3 approximately every 2 days. The battery of the FED3 was replaced every ~5 days. To avoid giving mice daily cyclic cues, we inspected the FED3 and mice at different times each day. The humidity and temperature inside the cabinet were 22.6 ± 0.5 °C (SD) and 47.7 ± 6.0 % (SD) during the experiment using wildtype mice and 22.4 ± 0.4 °C (SD) and 53.0 ± 2.2 % (SD) during the experiment using *Per1/2/3* KO mice. Double-plotted ethograms were generated by ClockLab analysis software (ver6.1.15, Actimetrics) in 6 min bins using the percentile plot with quantile 50. Although the percentile plot is best suited to provide a visual representation of complex patterns of rhythms, it does not provide actual values for the amounts of activity and other events. Therefore, we plotted averages of daily pellet intakes and numbers of left and right nose pokes in Figure S3.

For SCN *c-fos*-shGFP expression analysis, *c-fos*-shGFP reporter mice[26] were bred to *Per1/2/3* KO mice. Eight wildtype *c-fos*-shGFP mice (C57BL/6J background strain, 116 to 244-days-old females) and 16 *Per1/2/3* KO; *c-fos*-shGFP mice (C57BL/6J background strain, 55 to 128-days-old males and females) were individually housed in a small running wheel cage (11.5 cm W, 29.5 cm L, 12.0 cm H, wheel diameter 11.0 cm) and their wheel running activities were recorded as described above. After 12 to 14 days of recording, mice were anesthetized by Ketamine/Xylazine (20 mg/kg Ketamine; 16 mg/kg Xylazine) at middle of day (ZT6) or middle of night (ZT17), followed by immediate cardiac perfused with 0.01M phosphate buffer solution (PBS) and freshly prepared 4 % paraformaldehyde (PFA; Sigma-Aldrich, # 158127) in 0.01M PBS. Anesthesia at ZT17 was done under the

safe-red light (with Kodak GBX-2 filter) and perfusion was done under the room light. The brains were removed and post-fixed overnight in 4 % PFA in 0.01M PBS. Brains were cryoprotected with 30% sucrose (Crystalgen, # 300–777-1000) solution and embedded in O.C.T. compound (Tissue Plus, Fisher HealthCare, #4585), frozen, and stored at −80 °C until sectioned. 50 μm coronal sections containing the SCN were collected in PBS. A total of 3 coronal sections selected with every 3 consecutive sections (150 μm apart of 3 sections) from each individual were used for the analysis. All free float sections were stained by DAPI (1:1000 dilution; Roche #10236276001, Millipore Sigma) and mounted on glass slides with mounting media (ProLong Glass Antifade Mountant, Invitrogen, # P36980). Florescence images were captured by LSM880 (Zeiss) with 20X objective and frame scan mode. A single z image (1.4 μm optical section, 3 × 3 tile scan with 10% overlap and 1.3 zoom) was taken from each coronal slice. The same gain and laser power were used for all images (GFP: gain 556 and 2% laser power, DAPI gain 552 and 2.9% laser power).

QUANTIFICATION AND STATISTICAL ANALYSIS

Group average 24-h profiles were generated with 6 min bin data. For 3 days averaged 24-h profiles (Figure 1B), the individual 24-h daily profile was generated first by averaging 3 days of data in each condition, then mean and SEM among the individuals were determined. Therefore, SEM represents individual variability.

The onset of anticipatory poking and the onset of nocturnal activity were determined by the unbiased onset detection function in ClockLab. If ClockLab failed to detect the onset, we did not analyze the data as this would require a subjective method. Therefore, there are some missing data points, so we indicated sample sizes for each figure. We used ANOVA (mixed effects model to analyze repeated measures with missing values) followed by Dunnet’s test to compare the baseline phase with the phases for the few days after the treatment. Note that shifting the light-dark cycle results in one day of transition cycle. Although in advancing the light-dark cycle, the phase of the anticipatory poking and nocturnal activity is technically the same as the baseline (because those occurred before the change in light), we treated the transition day as a day in which the phase may be affected by the light cycle change in all conditions and thus compared baseline phase with other time points.

The cell count of the GFP positive cells was done with Image J (Fiji). 8bit gray scale of image were converted to binary images with the threshold of 15. The boarder of the SCN was determined by the DAPI signal. The total number of GFP positive cells within the bilateral SCN from 3 coronal sections in each mouse was determined blindly by the person who didn’t know the experimental conditions. A statistical difference between day and night was determined by Mann-Whitney U-test.

GraphPad Prism (version 10.0.2) was used for all statistical analysis as well as to calculate mean and SEM. All quantified data are plotted as mean ± SEM.

Supplementary Material

Refer to Web version on PubMed Central for supplementary material.

ACKNOWLEDGEMENTS

This work was supported by grants from the National Institutes of Health R01NS114527 and the National Science Foundation IOS-1931115 awarded to S.Y. D.E.E. is a postdoc scholar supported by National Institutes of Health T32 training grant (T32HL139438). The Neuroscience Microscopy Facility is supported by the UT Southwestern Neuroscience Department and the Peter O'Donnell Jr. Brain Institute. We thank Byeongha Jeong for FED3 programming and writing a code to convert FED3 data to readable format by ClockLab. We also would like to thank Julie S. Pendergast for reading the manuscript. Finally, we would like to thank the three anonymous reviewers who provided insightful comments and suggestions.

INCLUSION AND DIVERSITY

One or more of the authors of this paper self-identifies as an underrepresented ethnic minority in science. We support inclusive, diverse, and equitable conduct of research.

REFERENCES

1. Davidson AJ (2009). Lesion studies targeting food-anticipatory activity. Eur J Neurosci 30, 1658–1664. [PubMed: 19863659]
2. Mistlberger RE (2011). Neurobiology of food anticipatory circadian rhythms. Physiol Behav 104, 535–545. [PubMed: 21527266]
3. Pendergast JS, and Yamazaki S (2018). The Mysterious Food-Entrainable Oscillator: Insights from Mutant and Engineered Mouse Models. J Biol Rhythms 33, 458–474. 10.1177/0748730418789043. [PubMed: 30033846]
4. Richter CP (1922). A behavioristic study of the activity of the rat. Comp Psychol Monogr 1, 1–54.
5. Stephan FK (2002). The "other" circadian system: food as a Zeitgeber. J Biol Rhythms 17, 284–292. [PubMed: 12164245]
6. Mistlberger RE (1994). Circadian food-anticipatory activity: formal models and physiological mechanisms. Neurosci Biobehav Rev 18, 171–195. 10.1016/0149-7634(94)90023-x. [PubMed: 8058212]
7. Petersen CC, Cao F, Stinchcombe AR, and Mistlberger RE (2022). Multiple entrained oscillator model of food anticipatory circadian rhythms. Sci Rep 12, 9306. 10.1038/s41598-022-13242-w. [PubMed: 35661783]
8. Matikainen-Ankney BA, Earnest T, Ali M, Casey E, Wang JG, Sutton AK, Legaria AA, Barclay KM, Murdaugh LB, Norris MR, et al. (2021). An open-source device for measuring food intake and operant behavior in rodent home-cages. Elife 10. 10.7554/eLife.66173.
9. Kohsaka A, Laposky AD, Ramsey KM, Estrada C, Joshu C, Kobayashi Y, Turek FW, and Bass J (2007). High-fat diet disrupts behavioral and molecular circadian rhythms in mice. Cell Metab 6, 414–421. 10.1016/j.cmet.2007.09.006. [PubMed: 17983587]
10. Acosta-Rodriguez VA, de Groot MHM, Rijo-Ferreira F, Green CB, and Takahashi JS (2017). Mice under Caloric Restriction Self-Impose a Temporal Restriction of Food Intake as Revealed by an Automated Feeder System. Cell Metab 26, 267–277 e262. 10.1016/j.cmet.2017.06.007. [PubMed: 28683292]
11. Stephan FK, and Zucker I (1972). Circadian rhythms in drinking behavior and locomotor activity of rats are eliminated by hypothalamic lesions. Proc Natl Acad Sci U S A 69, 1583–1586. [PubMed: 4556464]
12. Rusak B (1977). Role of Suprachiasmatic Nuclei in Generation of Circadian-Rhythms in Golden-Hamster, Mesocricetus-Auratus. J Comp Physiol 118, 145–164. Doi 10.1007/Bf00611819.
13. Rusak B, and Zucker I (1979). Neural regulation of circadian rhythms. Physiol Rev 59, 449–526. [PubMed: 379886]
14. Eastman CI, Mistlberger RE, and Rechtschaffen A (1984). Suprachiasmatic nuclei lesions eliminate circadian temperature and sleep rhythms in the rat. Physiol Behav 32, 357–368. 10.1016/0031-9384(84)90248-8. [PubMed: 6463124]

15. Angeles-Castellanos M, Salgado-Delgado R, Rodriguez K, Buijs RM, and Escobar C (2010). The suprachiasmatic nucleus participates in food entrainment: a lesion study. Neuroscience 165, 1115–1126. 10.1016/j.neuroscience.2009.11.061. [PubMed: 20004704]

16. Pendergast JS, Oda GA, Niswender KD, and Yamazaki S (2012). Period determination in the food-entrainable and methamphetamine-sensitive circadian oscillator(s). Proc Natl Acad Sci U S A 109, 14218–14223. [PubMed: 22891330]

17. Verwey M, and Amir S (2009). Food-entrainable circadian oscillators in the brain. Eur J Neurosci 30, 1650–1657. 10.1111/j.1460-9568.2009.06960.x. [PubMed: 19863660]

18. Acosta-Galvan G, Yi CX, van der Vliet J, Jhamandas JH, Panula P, Angeles-Castellanos M, Del Carmen Basualdo M, Escobar C, and Buijs RM (2011). Interaction between hypothalamic dorsomedial nucleus and the suprachiasmatic nucleus determines intensity of food anticipatory behavior. Proc Natl Acad Sci U S A 108, 5813–5818. 10.1073/pnas.1015551108. [PubMed: 21402951]

19. Stephan FK (1992). Resetting of a feeding-entrainable circadian clock in the rat. Physiol Behav 52, 985–995. [PubMed: 1484856]

20. Stephan FK (1983). Circadian-Rhythm Dissociation Induced by Periodic Feeding in Rats with Suprachiasmatic Lesions. Behav Brain Res 7, 81–98. Doi 10.1016/0166-4328(83)90006-2. [PubMed: 6824529]

21. Stephan FK (1989). Entrainment of Activity to Multiple Feeding Times in Rats with Suprachiasmatic Lesions. Physiology & Behavior 46, 489–497. Doi 10.1016/0031-9384(89)90026-7. [PubMed: 2623075]

22. Stephan FK (1989). Forced Dissociation of Activity Entrained to T-Cycles of Food Access in Rats with Suprachiasmatic Lesions. J Biol Rhythm 4, 467–479. Doi 10.1177/074873048900400406.

23. Bae K, Jin X, Maywood ES, Hastings MH, Reppert SM, and Weaver DR (2001). Differential functions of mPer1, mPer2, and mPer3 in the SCN circadian clock. Neuron 30, 525–536. [PubMed: 11395012]

24. Shearman LP, Jin X, Lee C, Reppert SM, and Weaver DR (2000). Targeted disruption of the mPer3 gene: subtle effects on circadian clock function. Mol Cell Biol 20, 6269–6275. [PubMed: 10938103]

25. Flores DE, Bettilyon CN, and Yamazaki S (2016). Period-independent novel circadian oscillators revealed by timed exercise and palatable meals. Sci Rep 6, 21945. 10.1038/srep21945. [PubMed: 26904978]

26. Reijmers LG, Perkins BL, Matsuo N, and Mayford M (2007). Localization of a stable neural correlate of associative memory. Science 317, 1230–1233. 10.1126/science.1143839. [PubMed: 17761885]

Highlights

- Food-seeking nose poking is an output of the food-entrainable oscillator
- Nose pokes increase several hours before temporally restricted food availability
- Changing mealtime results in mice anticipating both the current and previous meals
- Anticipatory nose pokes entrain to the light in mice without a functional SCN

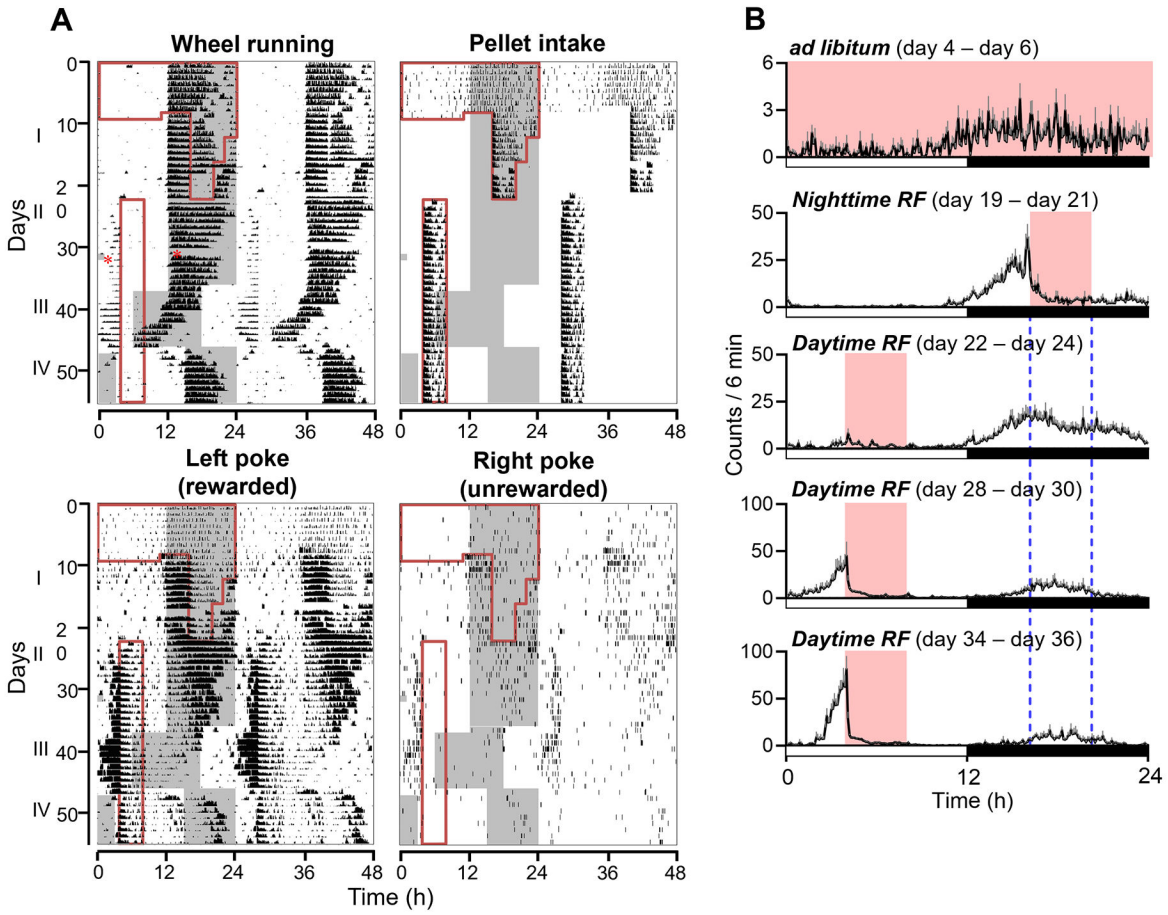

Figure 1. Predicted food availability is time-stamped on a light entrained circadian oscillator in wildtype mice.

(A) Representative double-plotted ethograms for wheel running activity, pellet intake, rewarded left nose pokes, and unrewarded right nose pokes recorded from one male C57BL/6N mouse (#2216). Ethograms of all 8 wildtype male mice are shown in Supplemental Figure S1. Dark (night) is indicated as gray shading, and the time of food availability is outlined in brown lines. These are indicated only on the left half of double plotted ethograms. Due to a technical issue (forced Windows update), ~12h running wheel data was not recorded (indicated by 2 red asterisks) and the mouse received a ~1 h dark pulse at the beginning of daytime on days 31–32. Because FED3 is battery-operated, this didn't affect data collection by FED3. The days when feeding or lighting conditions were changed are labeled with Roman numerals as follows: I: nighttime restricted feeding, II: daytime restricted feeding, III: 6 h advance of light-dark cycle, IV: 9 h delay of light-dark cycle. (B) Group average 24-h profiles of left nose poking before and after switching from nighttime restricted feeding to daytime restricted feeding. Mean activity profiles of rewarded left nose pokes in the last 3 days of *ad libitum* feeding, the last 3 days of nighttime restricted feeding, and the first 3 days, middle 3 days, and final 3 days of daytime restricted feeding are shown. Food availability (when pellets could be dispensed) is indicated with solid pink

boxes. Dotted blue vertical lines indicate onset and offset of the initial nighttime feeding. Data are presented as mean ± SEM. See also Figure S3 and S4.

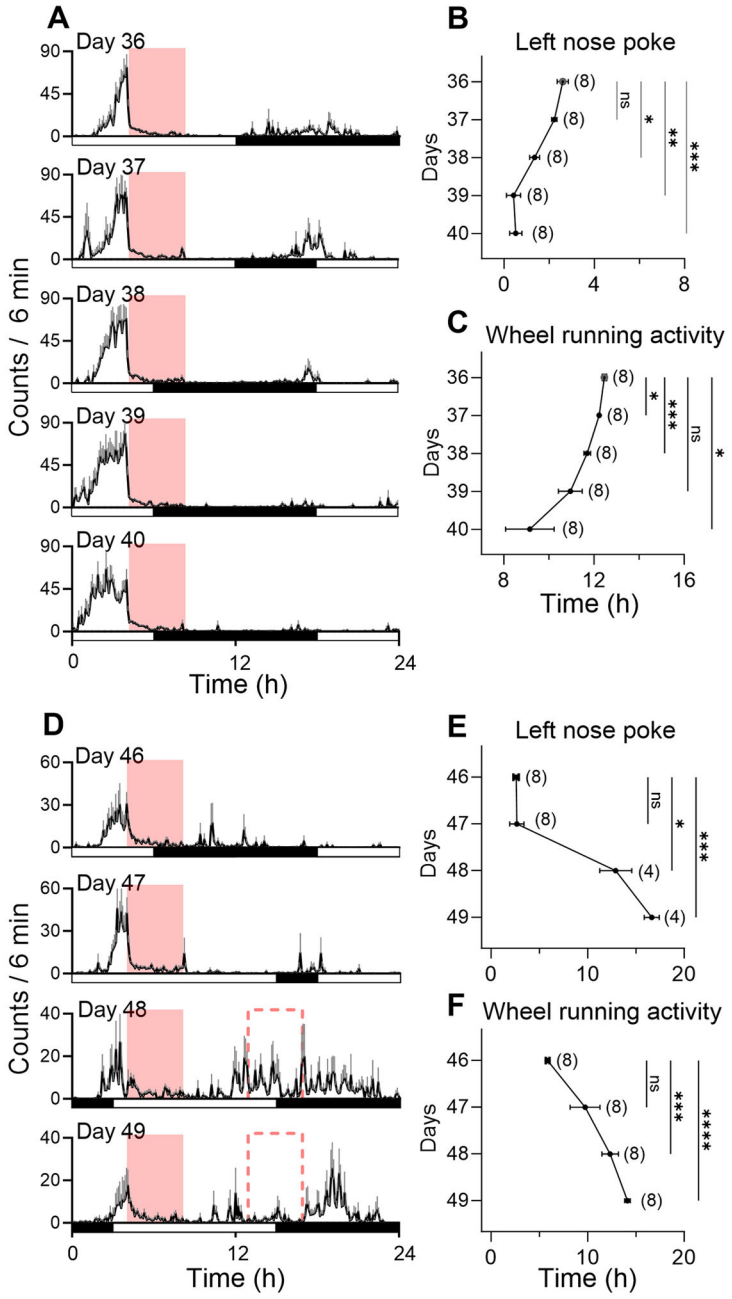

Figure 2. Food anticipatory nose pokes advance and delay with the light-dark cycle in wildtype mice.

(A) Group average daily profiles show mean rewarded left nose poking before (day 36) and after (days 38– 40) the advance of the light-dark cycle on day 37. (B) The onsets of left nose pokes and (C) wheel-running activity were determined in individual mice. (D) Group average daily profiles show mean rewarded left nose poking before (day 46) and after (days 48, 49) the delay of the light-dark cycle on day 47. (E) The onsets of left nose pokes and (F) wheel-running activity were determined in individual mice. Pink shaded boxes show the time of food availability. Pink dotted lines indicate the time of food availability

if it is linked to the phase of a light-entrainable oscillator. *p<0.05, **p<0.01, ***p<0.001, ****p<0.0001; ns, not significant. Data presented as mean ± SEM. Sample size (number of onsets which could be determined by ClockLab) is indicated in brackets, see quantification and statistical analysis. See also Figure S3 and S4.

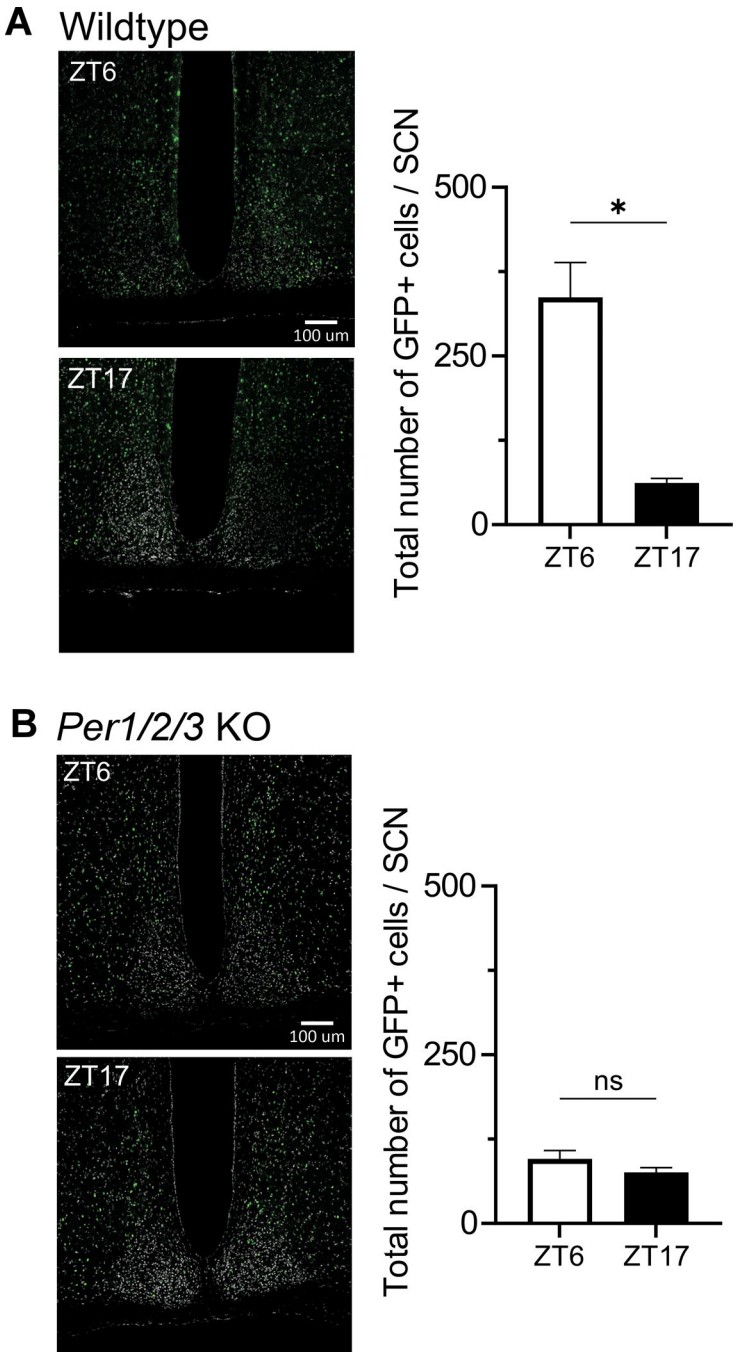

Figure 3. There is no day-night difference in the expression of *c-fos*-shGFP in the *Per1/2/3* KO SCN.

Representative *c-fos*-shGFP expression in the SCN at middle of day (ZT6) and middle of night (ZT17) in wildtype (A) and *Per1/2/3* KO (B) mice. DAPI: gray scale, GFP: green. Total number of GFP positive SCN cells of 3 coronal sections per animal were counted. Data are presented as mean ± SEM. *p<0.05 by Mann-Whitney U-test; ns, not significant. WT ZT6 (4 females), WT ZT17 (4 females), *Per1/2/3* KO ZT6 (4 males, 4 females), *Per1/2/3* KO ZT17 (4 males, 4 females). See also Figure S4.

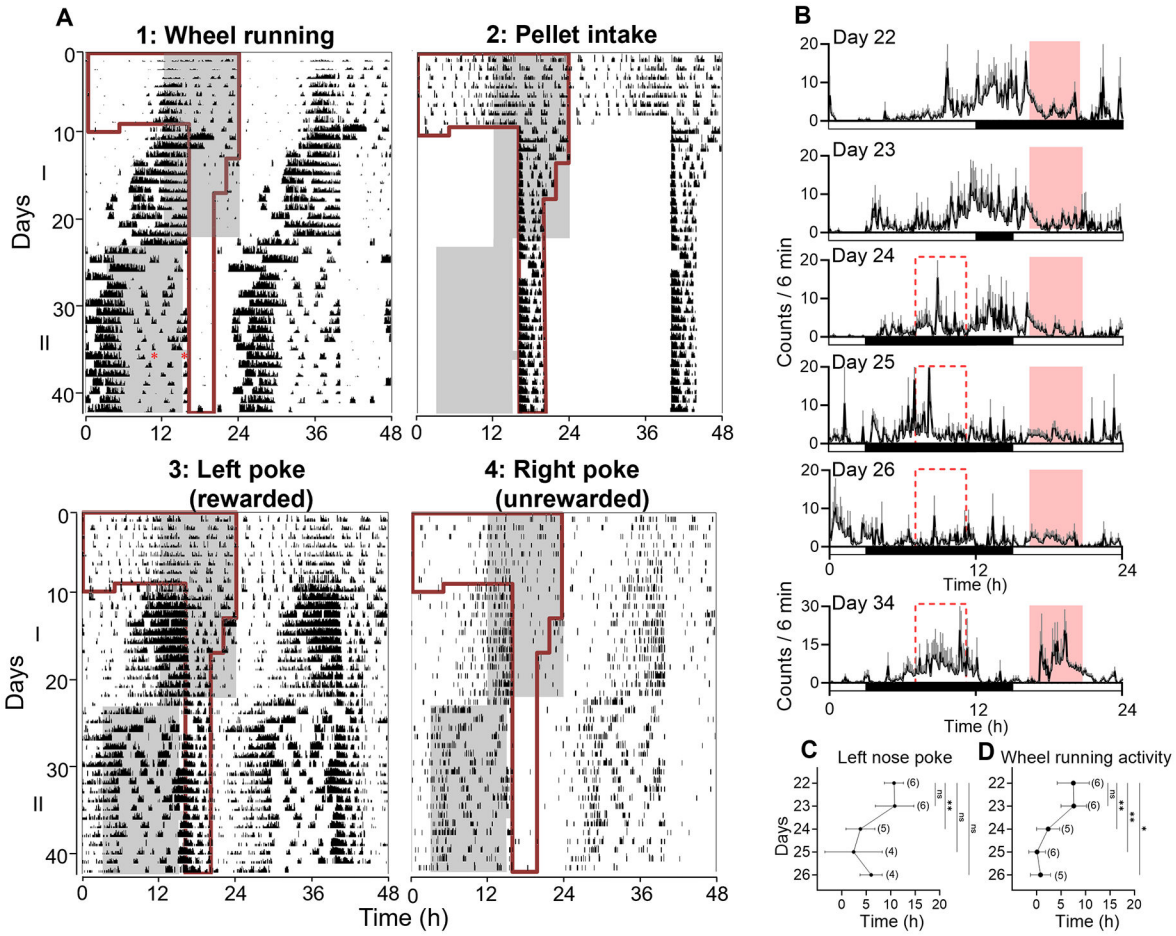

Figure 4. Anticipatory nose pokes rapidly advance with the light-dark cycle in *Per1/2/3* KO mice that have nonfunctional SCN.

Per1/2/3 KO mice were fed *ad libitum* for 9 days and then fed with timed restriction. At 13 days of nighttime restricted feeding, the light-dark cycle was advanced by 9h, while feeding time was kept unchanged. (A) Representative double-plotted ethograms of wheel running activity, pellet intake, rewarded left nose pokes, and unrewarded right nose pokes recorded from one male *Per1/2/3* KO mouse (#11500). Ethograms of all 6 male *Per1/2/3* KO mice are shown in Supplemental Figure S2. Due to a technical issue (forced Windows update), ~4h running wheel data was not recorded (indicated by 2 red asterisks) and the mouse received a ~1 h dark pulse at the beginning of daytime on day 36. Because FED3 is battery-operated, this didn't affect data collection by FED3. The days when feeding or lighting conditions were changed are labeled with Roman numerals as follows: I: nighttime restricted feeding, II: 9h advance of light-dark cycle. (B) Group average daily profiles show mean rewarded left nose poking before (day 22) and after (days 24–26 and 34) the advance of the light-dark cycle on day 23. (C) The onsets of left nose pokes and (D) wheel-running activity were determined in individual mice. Pink shaded boxes show the time of food availability. Pink dotted lines indicate the time of food availability if it is linked to the phase of a light-entrainable oscillator. *p<0.05, **p<0.01; ns, not significant. Data presented as

mean ± SEM. Sample size (number of onsets which could be determined by ClockLab) is indicated in brackets, see quantification and statistical analysis. See also Figure S3 and S4.

Key resources table

REAGENT or RESOURCE	SOURCE	IDENTIFIER
Antibodies		
Bacterial and virus strains		
Biological samples		
Chemicals, peptides, and recombinant proteins		
Paraformaldehyde	Sigma-Aldrich	158127
30% sucrose solution	Crystalgen	300–777-1000
O.C.T. compound (Tissue Plus)	Fisher HealthCare	4585
DAPI	Roche	10236276001
ProLong Glass Antifade Mountant	Invitrogen	P36980
Critical commercial assays		
Deposited data		
Raw data	This paper	DOI: 10.17632/cr5hkkdtx2.1
Experimental models: Cell lines		
Experimental models: Organisms/strains		
Mouse: B6.129-Per1^{tm1Drw}/J	The Jackson Laboratory	JAX: 010491
Mouse: B6.129-Per2^{tm1Drw}/J	The Jackson Laboratory	JAX: 010492
Mouse: B6.129S4-Per3^{tm1Drw}/J	The Jackson Laboratory	JAX: 010493
Mouse: B6.Cg-Tg(Fos-tTA,Fos-EGFP*)1Mmay/J	The Jackson Laboratory	JAX: 018306
Mouse: C57BL/6NCrL	Charles River	Charles River: 027
Oligonucleotides		
Recombinant DNA		

REAGENT or RESOURCE	SOURCE	IDENTIFIER
Software and algorithms		
ClockLab Data Collection (ver. 3.604)	Actimetrics	https://actimetrics.com/products/clocklab
ClockLab Chamber Control (ver. 4.104)	Actimetrics	https://actimetrics.com/products/clocklab
ClockLab Analysis Software (version 6.1.15)	Actimetrics	https://actimetrics.com/products/clocklab/
GraphPad Prism (version 10.0.2)	Dotmatics	https://www.graphpad.com/
Fiji Image J (version 1.54b)	N/A	https://imagej.net/software/fiji/downloads
Python (version 3.11.4)	N/A	https://www.python.org/
Arduino IDE (version 2.1.1)	N/A	https://www.arduino.cc/en/software
Other		
FED3 – feeding device	LABmaker	FED3
20 mg food pellet	Bio-Serv	F0163
Red safelight filter	Kodak	GBX-2
FED3 code	This paper	DOI: 10.17632/cr5hkkdtx2.1
Python code for FED3 data conversion	This paper	DOI: 10.17632/cr5hkkdtx2.1